Materials Science-Poland, 35(4), 2017, pp. 885-892
http://www.materialsscience.pwr.wroc.pl/
DOI: 10.1515/msp-2017-0108

DE GRUYTER OPEN

Investigation of dielectric properties of heterostructures based on ZnO structures

A.H. SELÇUK[1], E. ORHAN[2], S. BILGE OCAK[3,*], A.B. SELÇUK[4], U. GÖKMEN[3]

[1]Balıkesir University, Faculty of Engineering Department of Electric and Electronic Engineering, 10145, Balıkesir, Turkey
[2]Gazi University, Faculty of Science, Department of Physics, 06500 Ankara, Turkey
[3]Gazi University, Graduate School of Natural and Applied Science, Department of Advanced Technology, 06500 Ankara, Turkey
[4]İzmir Democracy University, Faculty of Engineering, Department of Biomedical Engineering, 35140 İzmir, Turkey

The voltage and frequency dependence of dielectric constant ϵ', dielectric loss ϵ'', electrical modulus M'', M', loss tangent tanδ and AC electrical conductivity σ_{AC} of p-Si/ZnO/PMMA/Al, p-Si/ZnO/Al and p-Si/PMMA/Al structures have been investigated by means of experimental G-V and C-V measurements at 30 kHz, 100 kHz, 500 kHz and 1 MHz in this work. While the values of ϵ', ϵ'', tanδ and σ_{AC} decreased, the values of M' and M'' increased for these structures when frequency was increased and those of p-Si/ZnO/Al and p-Si/PMMA/Al were comparable with those of p-Si/ZnO/PMMA/Al. The obtained results showed that the values of p-Si/ZnO/PMMA/Al structure were lower than the values of p-Si/ZnO/Al and p-Si/PMMA/Al.

Keywords: *electric modulus; organic thin film; dielectric loss; heterostructure; electrical conductivity*

1. Introduction

Because of its large exciton binding energy (60 meV) and direct bandgap energy (3.37 eV), the applications of heterostructure based on zinc oxide attracted great interest. Many applications involve this material in the forms of thin film solar cells [1], transparent conducting electrodes [2], light-emitting diodes (LEDs) and ultraviolet (UV) photodetectors [3]. Different fabrication techniques are used to grow ZnO on various substrates such as reactive evaporation [4], chemical vapor deposition (HVP-CVD) [5], sol-gel spin coating method [6], spray pyrolysis [7] and magnetron sputtering [8] for the heterojunction structures [9]. Heterostructures have scientific and commercial significance and they are a basic type of semiconductor, electronic and optoelectronic devices. Metal coated polymer materials used as an interfacial layer can reduce interdiffusion at metal/semiconductor (MS) interface that has a negative effect on electronic characteristics. So, organic and inorganic heterostructures became attractive to be used in semiconductor devices [10–15].

Imaginary and real parts of dielectric loss and loss tangent are strongly affected by metal or polymers coated on the structures [16–19]. It is known that PMMA has chemical sensing capability, good insulation properties, high rigidity, transparency, dielectric constant and capability of collection of negative charges.

The interface states, ideality factor, series resistance and barrier height of p-Si/PMMA/Al, p-Si/ZnO/Al and p-Si/ZnO/PMMA/Al heterostructures were calculated from the measurements of the I-V and C-V characteristics in our previous work [19].

It was found that the p-Si/ZnO/PMMA/Al structure shows better electronic performance than the others. PMMA heterostructure with ZnO coating has changed the electrical parameters of p-Si/PMMA/Al and p-Si/ZnO/Al structures. Although many aspects of the performance of heterostructure devices are quite well understood, there are properties which are still a subject of

*E-mail: sbocak@gazi.edu.tr; semabilge72@gmail.com

© 2017. This is an open access article distributed under the Creative Commons Attribution-NonCommercial-NoDerivatives 3.0 License.
(http://creativecommons.org/licenses/by-nc-nd/3.0/)

worldwide studies. There is a remarkable lack of knowledge, especially in terms of interfacial interactions of heterostructures. Much more studies on the quantitative characterization of effective interface interactions seem to be needed. It is essential to investigate both the dielectric properties of the heterostructures and the interactions between interfaces.

Dielectric properties of dipoles are very important for the interface. Generally, the polarizations of dipoles are classified into four groups as atomic/ionic (α_a) polarization, electron (α_e) polarization, interface (α_i) polarization and oriental/dipolar (α_o) polarization [20–26]. Material polarization is one of these polarization mechanisms with a short range motion of the charge.

While atomic polarization can be observed in the range of $10^{10} < f < 10^{13}$ Hz, electronic polarization may appear at $f > 4 \times 10^{15}$ Hz. However, dipolar polarization may occur in high or intermediate frequency range of 1 kHz to 1 MHz because of the longer relaxation time and may result from the location of surface charges, impurities, orientable dipoles [24–26]. The interfacial polarization at $f < 10^{13}$ Hz is principally more sensitive [27]. In particular, when a physical barrier that inhibits charge migration impedes mobile charge carriers, the interfacial polarization occurs. Therefore, the charges are accumulated in the barriers producing localized polarization in the material [27].

After examining the I-V and C-V properties of p-Si/PMMA/Al, p-Si/ZnO/Al and p-Si/ZnO/PMMA/Al, the voltage and frequency dependent dielectric properties of these heterostructures should be investigated. In the present work, the dielectric properties of these heterostructures are described by C-V and G-V measurements at 30 kHz, 100 kHz, 500 kHz and 1 MHz. The variations of AC electrical conductivity σ_{AC}, imaginary and real parts of electric modulus M'' and M', dielectric constant ϵ', dielectric loss ϵ'' and loss tangent $\tan\delta$ are investigated.

2. Experimental

The structures were fabricated on p-type Si (1 1 1) wafers having 10 ohm resistivity and 280 μm thickness. Chemical cleaning procedures described previously in detail were applied to the wafer [19, 20]. Then it was put inside a vacuum chamber to form a good ohmic contact with a thickness of 1240 Å on unpolished surface using Al (99.999 %). After that, the wafer was annealed at 500 °C in vacuum for 10 minutes to dope aluminum into the back surface of it. The whole back side was coated by Al (99.999 %) to obtain a good ohmic contact and it was cut into three pieces. Two of them were coated by ZnO and one was left as non-coated. Next, ZnO was obtained by evaporation at a pressure of 2.66×10^{-4} Pa and annealed at 405 °C in atmospheric conditions for 4 minutes. PMMA layer was deposited on all the pieces by spin coating technique. The spin coating was performed at 5000 rpm for 45 seconds on polished surface of the wafer and then the wafer was heated to 180 °C for 60 seconds. Finally, rectifying contacts were deposited on all three wafers by evaporation technique at 2.66×10^{-4} Pa pressure using high purity circular Al dots having 1280 Å thickness and 1.3 mm diameter. In this way, all three structures were made nearly in the same conditions. C-V and G-V measurements were carried out at room temperature to measure the dielectric characteristics of the structures in darkness. Thicknesses of PMMA and oxide layers were evaluated by a thickness monitor and an ellipsometer as 10 nm and 20 nm, respectively.

3. Results and discussion

Using the values of G and C of p-Si/PMMA/Al, p-Si/ZnO/Al and p-Si/ZnO/PMMA/Al heterostructures at different frequencies (30 kHz, 100 kHz, 500 kHz and 1 MHz), applied voltage dependence of ϵ'', ϵ', σ_{AC} and $\tan\delta$ of ZnO, PMMA and ZnO/PMMA interfaces have been studied. While the imaginary part of dielectric constant indicates the energy losses owing to conduction and polarization, the real part indicates the polarizability or capacitive behavior of a material. The complex

permittivity formula is used to define dielectric and electric properties and it can be introduced using the following expressions:

$$\varepsilon^* = \varepsilon' - i\varepsilon'' \tag{1}$$

$$\varepsilon' = \frac{C}{C_0} = \frac{Cd_p}{\varepsilon_0 A} \tag{2}$$

$$\varepsilon'' = \frac{d_p G}{A\varepsilon_0 \omega} \tag{3}$$

where i is the square root of -1, C_0 is capacitance of an empty capacitor, G and C are the measured admittance and conductance values, d_p is the interfacial insulator layer thickness, ϵ_0 is the permittivity of free space charge, $(\omega = 2\pi f)$ is the angular frequency and A is the rectifying contact area of the structure in cm^2. The value of tanδ can be calculated as follows:

$$\tan\delta = \frac{\varepsilon''}{\varepsilon'} \tag{4}$$

The σ_{AC} of the dielectric material is expressed as follows [28, 29]:

$$\sigma_{AC} = 2\pi f \varepsilon_0 \varepsilon' \tan\delta \tag{5}$$

Dielectric properties of materials can be expressed in various forms using different notations. Several authors have discussed the complex terms of electric modulus (M^*) and impedance (Z^*) of polymer or dielectric materials. In defining conduction mechanisms of these materials, the electric modulus and dielectric properties have been preferred by most authors. In order to describe the bulk DC conductivity of a material and to separate the bulk and the surface phenomena, analysis of ϵ^* data in Z^* formula is commonly preferred. ϵ^* is converted to the M^* formula as follows:

$$M^* = iwC_0 Z^* \tag{6}$$

or

$$M^* = \frac{1}{\varepsilon^*} = M + jM'' = \frac{\varepsilon'}{\varepsilon'^2 + \varepsilon''^2} + j\frac{\varepsilon'}{\varepsilon'^2 + \varepsilon''^2} \tag{7}$$

M'' and M' are computed from ϵ'' and ϵ'.

As may be seen in Fig. 1, the real part of ϵ^* depends on the voltage of p-Si/PMMA/Al, p-Si/ZnO/Al and p-Si/ZnO/PMMA/Al heterostructures at various frequencies. For the dielectric material, variations in ϵ' with voltage for all three types of the structures display normal behavior. As electronic, dipolar and atomic contributions influence the dielectric constant at lower frequencies, only atomic polarization and dipolar contributions remain at high frequency owing to the fact that the electronic polarization reduces with increasing frequency. It is pointed out that the values of ϵ' tend to be frequency independent at low voltages and decrease with increasing frequency. The decrease in ϵ' with increasing frequency is connected with polarization decrease with increasing frequency, and it tends to a constant value. The dispersion in ϵ' with frequency, ascribed to Maxwell-Wagner type interfacial polarization, i.e. ϵ'' versus voltage of p-Si/PMMA/Al, p-Si/ZnO/Al and p-Si/ZnO/PMMA/Al at various frequencies, is seen in Fig. 2. As shown in Fig. 2, ϵ'' decreases exponentially for all structures. Dissipation of p-Si/PMMA/Al is much higher than that of p-Si/ZnO/PMMA/Al and p-Si/ZnO/Al structures. This can be related to defects present in the film generating potential barrier and interfaces or grain boundaries. ϵ'' depends on space charge polarization with dipolar effects at lower frequencies.

The plots of tanδ versus voltage for p-Si/PMMA/Al, p-Si/ZnO/Al and p-Si/ZnO/PMMA/Al structures at various frequencies are shown in Fig. 3. The values of tanδ have small peaks and they shift towards right with increasing voltages at high frequency region. This behavior of tanδ may be clarified by the equality of the hopping frequency of charge carriers and that of the external applied field. The degree of polarization and value of frequency describe the dielectric relaxation process [30, 31]. The probabilities of these space charges to accumulate and drift at the interface become very low as an electric field at high frequency is applied. Generally, the occurrence of interfacial polarization is observed at lower frequencies. Its occurrence in a system is generally related to distinct variations in the trends of tanδ

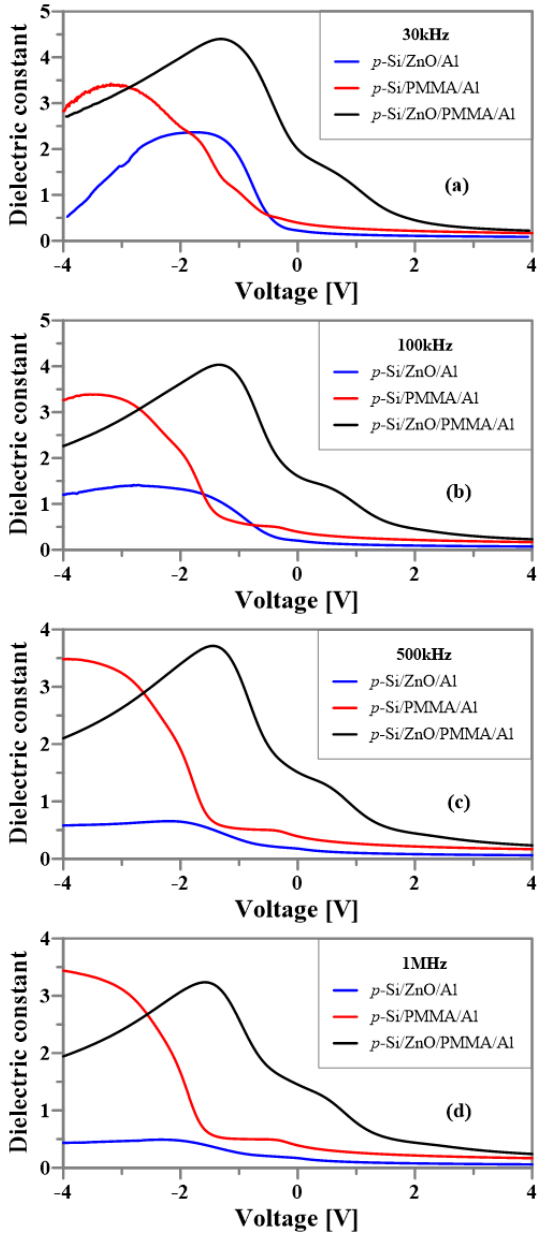


Fig. 1. Dielectric constant ϵ' as a function of applied voltage at room temperature (a) at 30 kHz (b) at 100 kHz (c) at 500 kHz (d) at 1 MHz.

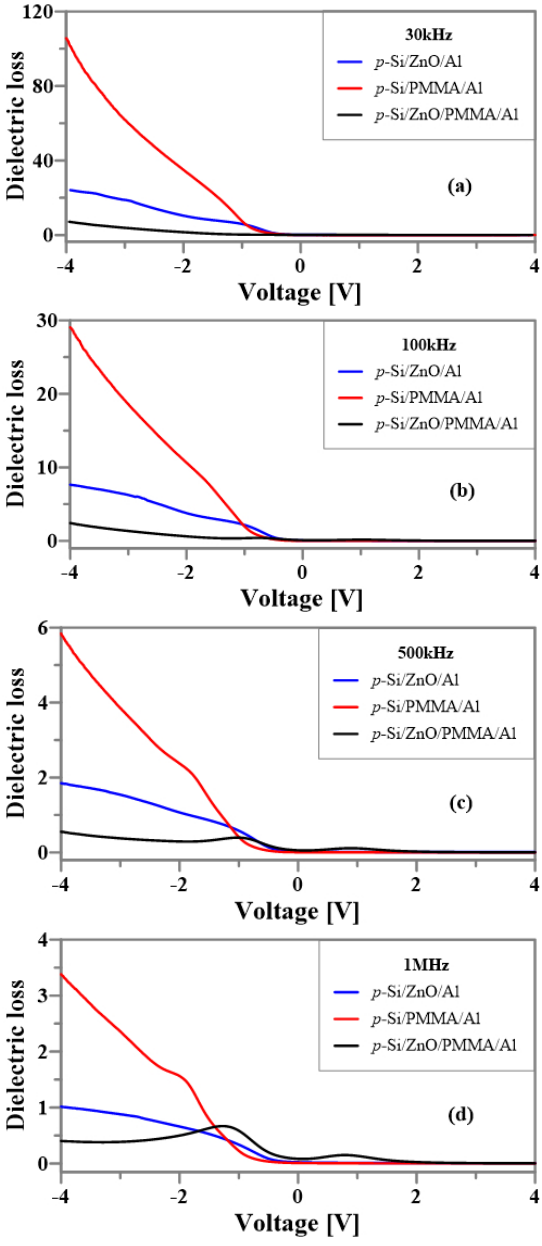


Fig. 2. Dielectric loss ϵ'' as a function of applied voltage at room temperature (a) at 30 kHz (b) at 100 kHz (c) at 500 kHz (d) at 1 MHz.

and effective permittivity with respect to frequency owing to the fact that interfacial phenomena have an additional polarization mechanism besides dipolar, electronic and ionic [31].

The σ_{AC}-V plots were also obtained from the conductivity data and are given in Fig. 4. As shown in Fig. 4, the σ_{AC} conductivity is strongly frequency dependent. The decrease in electrical conductivity causes a decrease in the eddy currents. Therefore, tanδ is decreased.

The M' and M'' values were calculated from ϵ' and ϵ''. Fig. 5 and Fig. 6 show the voltage dependence of real (M') and imaginary (M'') parts of the electric modulus for p-Si/PMMA/Al, p-Si/ZnO/Al

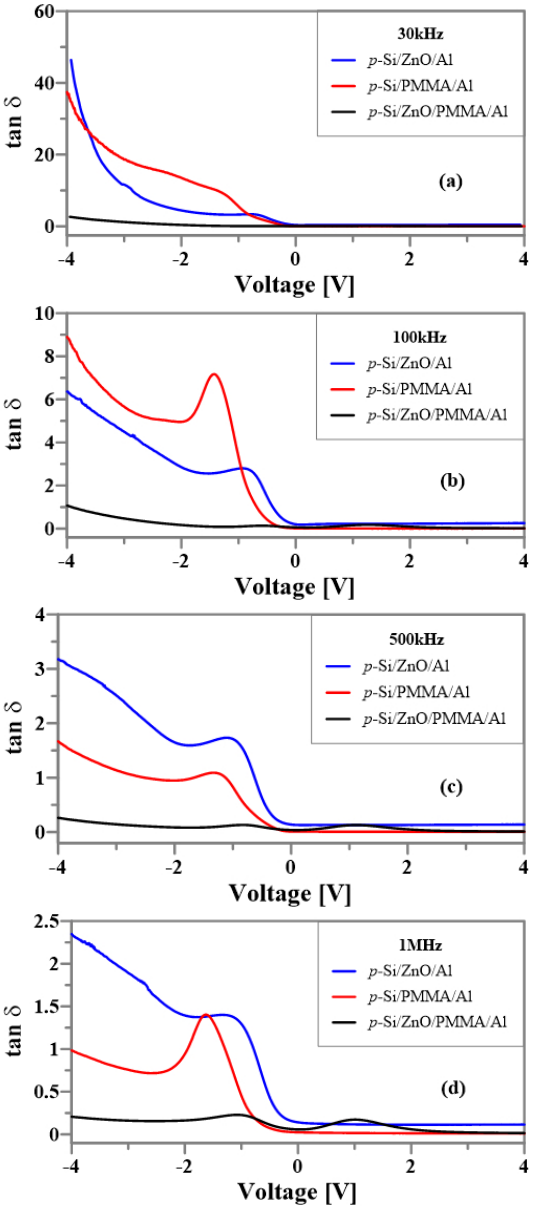


Fig. 3. The tangent loss tanδ as a function of applied voltage at room temperature (a) at 30 kHz (b) at 100 kHz (c) at 500 kHz (d) at 1 MHz.

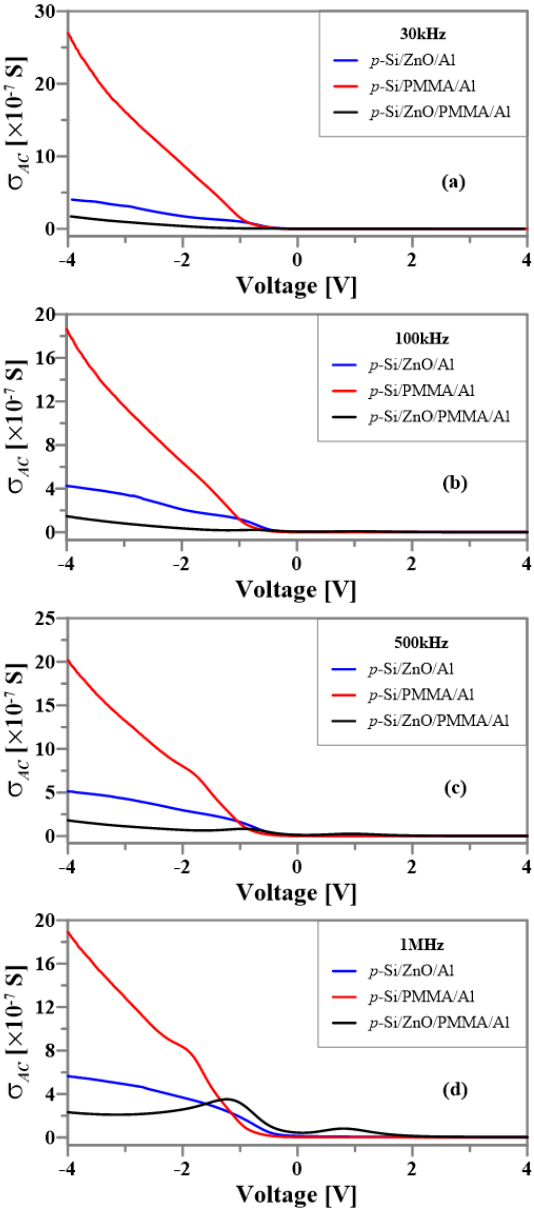


Fig. 4. AC electrical conductivity σ_{AC} as a function of applied voltage at room temperature (a) at 30 kHz (b) at 100 kHz (c) at 500 kHz (d) at 1 MHz.

and p-Si/ZnO/PMMA/Al structures at various frequencies. As seen in Fig. 5 and Fig. 6, the values of M' and M'' decrease with decreasing frequency. This behavior may be referred to the polarization increase with increasing frequency for all three structures [31]. In other words, M' reaches a constant maximum value $M_\infty = 1/\epsilon_\infty$ because of the relaxation process.

Owing to the fact that electron polarization does not exist at low frequencies, the values of M' approach zero. Fig. 5 indicates that M' increases exponentially with increasing voltage at all frequencies. It is seen from Fig. 6 that M'' has a peak at all studied frequencies and the peak shifts to the lower voltages with increasing frequency. It has been

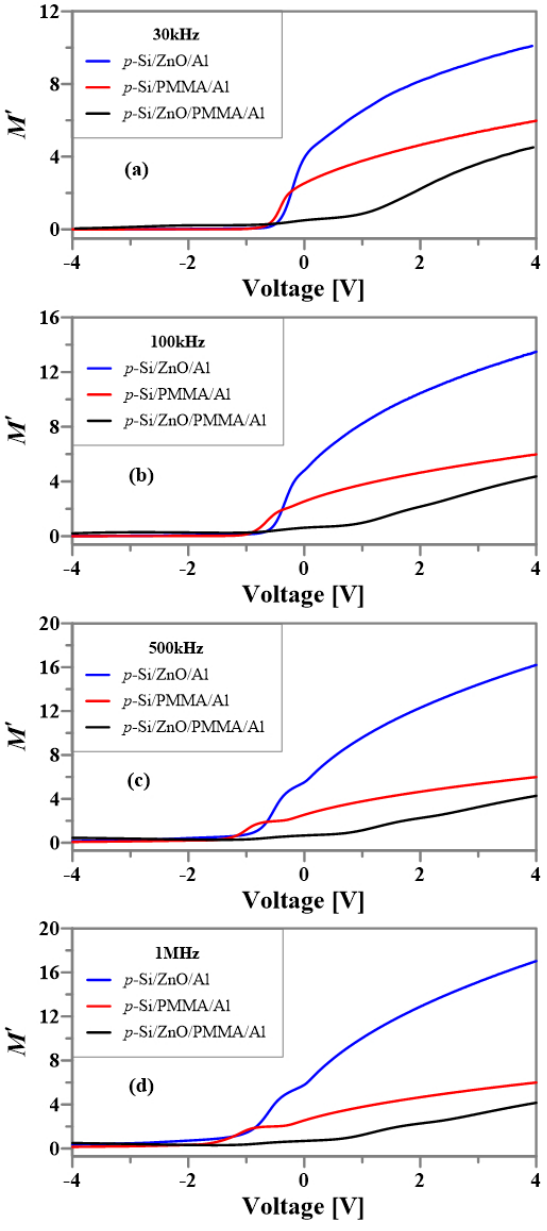


Fig. 5. The real part of the dielectric loss modulus M′ as a function of applied voltage at room temperature (a) at 30 kHz (b) at 100 kHz (c) at 500 kHz (d) at 1 MHz.

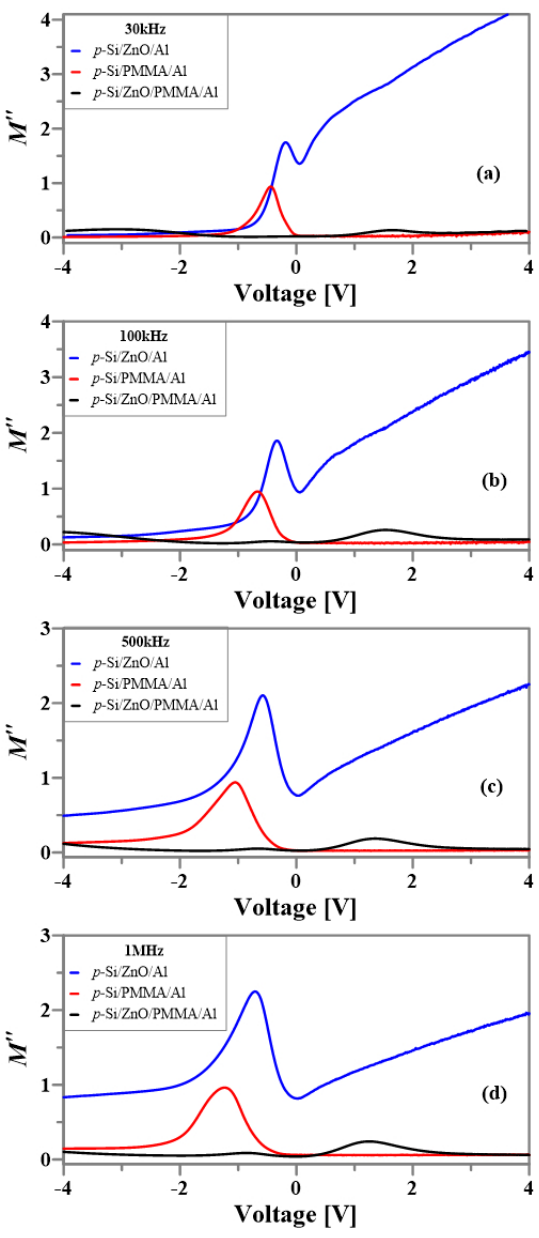


Fig. 6. The imaginary part of the dielectric loss modulus M″ as a function of applied voltage at room temperature (a) at 30 kHz (b) at 100 kHz (c) at 500 kHz (d) at 1 MHz.

reported that increasing frequency causes an increase in relaxation times and the energy of charge carrier [31]. The dispersion of relaxation times depends on the grain boundaries and various grains in all three structures [27–31]. The behavior of one peak in M″ may result from the existence of a particular density distribution profile of interface states at all three interfaces. All charges at interface states/traps can easily follow an external AC signal at low frequencies and this explains the excessive capacitance and conductance. The change in σ_{AC}, M″ and M′ is a result of reordering and restructuring of charges at the interface under polarization and voltage or external electric field. The values of

ϵ' and ϵ'' at high frequencies are not contributed from interface states, so the capacitance is small. Therefore, these structures may be used in high frequency applications. Electrical conductivity contributes only to the dielectric loss. The increase in electrical conductivity leads to a current loss, thus tanδ increases. As ϵ' of p-Si/ZnO/PMMA/Al structure is higher than those of p-Si/PMMA/Al and p-Si/ZnO/Al devices at all frequencies, ϵ'', σ_{AC}, M'', tanδ and M' of p-Si/ZnO/PMMA/Al structures are smaller than those of p-Si/PMMA/Al, p-Si/ZnO/Al devices due to the existence of a thin organic layer and ZnO oxide.

4. Conclusions

We fabricated and analyzed the dielectric characteristics of p-Si/PMMA/Al, p-Si/ZnO/Al and p-Si/ZnO/PMMA/Al structures at various frequencies. It is shown that the dispersions in ϵ', ϵ'', tanδ, M'', M' and σ_{AC} values of the structures are dependent on the applied bias voltage in depletion region and they are remarkably high at low frequencies. Debye relaxation model for interfacial polarization together with dipole and interface states effect explain the strong decrease in ϵ' and ϵ'' with increasing frequency. The decrease in ϵ' and ϵ'' with increasing frequency are observed for all operating voltages. ϵ' and ϵ'' values at high frequencies are not contributed from interface states since the capacitances of these diodes are small, therefore these structures may be used in high frequency applications. As a consequence, it has been found that the all values of p-Si/ZnO/PMMA/Al structure except ϵ' are smaller than those of p-Si/PMMA/Al and p-Si/ZnO/Al devices due to the existence of organic layers and a thin ZnO oxide.

Acknowledgements

This work is financially supported by the Gazi University Scientific Research Project (Project Number: 65/2017-01).

References

[1] SHIN B.K., LEE T.I., XIONG J., HWANG C., NOH G., CHO J.H., MYOUNG J.M., *Sol. Energ. Mat. Sol. C.*, 95 (2011), 2650.

[2] OOTSUKA T., LIU Z., OSAMURA M., FUKUZAWA Y., KURODA R., SUZUKI Y., OTOGAWA N., MISE T., WANG S., HOSHINO Y., NAKAYAMA Y., TANOUE H., MAKITA Y., *Thin Solid Films*, 476 (2005), 30.

[3] SZARKO J.M., SONG J.K., BLACKLEDGE C.W., SWART I., LEONE S.R., LI S., ZHAO Y., *Chem. Phys. Lett.*, 404 (2005), 171.

[4] ASMAR AL R., ATANAS J.P., AJAKA M., ZAATAR Y., FERBLANTIER G., SAUVAJOL J.L., JABBOUR J., JUILLAGET S., FOUCARAN A., *J. Cryst. Growth*, 279 (2005), 394.

[5] BARNES T.M., LEAF J., HAND S., FRY C., WOLDEN C.A., *J. Cryst. Growth*, 274 (2004), 412.

[6] CHEN S., ZHANG J., FENG X., WANG X., LUO L., SHI Y., XUE Q., WANG C., ZHU J., ZHU Z., *Appl. Surf. Sci.*, 241 (2005), 384.

[7] AYOUCHI R., LEINEN D., MARTIN F., GABAS M., DALCHIELE E., RAMOS-BARRADO J.R., *Thin Solid Films*, 426 (2003), 68.

[8] CHAABOUNI F., ABAAB M., REZIG B., *Superlattice. Microst.*, 39 (2006), 171.

[9] SELIM OCAK Y., *J. Alloy. Compd.*, 513 (2012), 130.

[10] KOIDE Y., *Appl. Surf. Sci.*, 254 (2008), 6268.

[11] CAPUTO D., CESARE DE D., NASCETT A., TUCCI M., *Sensor. Actuat. A-Phys.*, 153 (2009), 1.

[12] GRAMSCH E., PCHELYAKOV O.P., CHISTOKHIN I. B., THISHKOVSKY G., *IEE T. Electron. Dev.*, 54 (2007), 2638.

[13] JIN Y., WANG J., SUN B., BLAKESLEY J.C., GREENHAM N.C., *Nano Lett.*, 8 (2008), 1649.

[14] ZHAI T., FANG X., LIAO M., XU X., LIANG LI., LIU B., KOIDE Y., MA Y., YAO J., BANDO Y., GOLBERG D., *ACS Nano.*, 4 (2010), 1596.

[15] LEUNG Y.H., HE Z.B., LUO L.B., TSANG C.H.A., WONG N.B., ZHANG W.J., LEE S.T., *Appl. Phys. Lett.*, 96 (2010), 053102.

[16] HE J.H., HSU J.H., WANG C.W., LIN H.N., CHEN L.J., WANG Z.L., *J. Phys. Chem. B.*, 110 (2006), 50.

[17] SUN X.W., HUANG J.Z., WANG J. X., XU Z., *Nano Lett.*, 8 (4) (2008), 1219.

[18] BILGE OCAK S., SELÇUK A.B., ARAS G., ORHAN E., *Mat. Sci. Semicon. Proc.*, 38 (2015), 249.

[19] SELÇUK A.B., BILGE OCAK S., ARAS F.G., OZ ORHAN E., *J. Electron. Mater.*, 43 (2014), 3263.

[20] SCHULZ M., KLAUSMANN E., *J. Appl. Phys.*, 18 (1979), 169.

[21] KONOFAOS N., MC CLEAN I.R., THOMAS C.B., *Phys. Status Solidi A.*, 161 (1997), 111.

[22] BILGE OCAK S., SELÇUK A.B., ARAS G., ORHAN E., *Mat. Sci. Semicon. Proc.*, 38 (2015), 249.

[23] AFANDIYEVA I.M., ASKEROV SH.G., ABDULLAYEVA L.K., ASLANOW SH.S., *Solıd State Electron.*, 51 (2007), 1096.

[24] FARUK YÜKSEL Ö., SELCUK A.B., OCAK S.B., *Vacuum*, 82 (2008), 1183.

[25] SYMTH C.P., *Dielectric Behaviour and Structure*, McGraw-Hill, New York, 1995.

[26] POPESCU M., BUNGET I., *Physics of Solid Dielectrics*, Elsevier, Amsterdam, 1984.

[27] KWA K.S., CHATTOPADHYAY S., JANCOVIC N.D., OLSEN S.H., DRISCOLL L.S., O'NIELL A.G., *Semicond. Sci. Tech*., 18 (2003), 82.

[28] FAIVRE A., NIQUET G., MAGLIONE M., FORNAZERO J., LAI J.F., DAVID L., *Eur. Phys. J. B*, 10 (1999), 277.

[29] PISSIS P., KIRITSIS A., *Solid State Ionics*, 97 (1997), 105.

[30] MIGAHED M.D., ISHRA M., FAHMY T., BARAKAT A., *J. Phys. Chem. Solids*, 65 (2004), 1121.

[31] CHATTOPHADHYAY A., RAYCHAUDHURI B., *Solid State Electron.*, 35 (1992), 875.

Received 2017-07-26
Accepted 2017-12-07